An 11 - year global 3D climatology and trends of aerosol optical depth using satellite data from CALIOP

Anastasia Kakouri[1,3], Marios Bruno Korras Carraca[1], Themistoklis Kontos[1], Christos Matsoukas[1], Nikolaos Hatzianastassiou[2], Athina Avgousta Floutsi[4] and Effie Kostopoulou[3]

[1]Department of Environment, University of the Aegean, Mytilene, Greece
[2]Laboratory of Meteorology, Department of Physics, University of Ioannina, Ioannina, Greece
[3]Department of Geography, University of the Aegean, Mytilene, 811 00, Greece
[4]Leibniz Institute for Tropospheric Research, Permoserstraße 15, 04318 Leipzig, Germany

Keywords:GIS, Remote Sensing, climate change, trend analysis, vertical profiles, aerosols
Presenting author email: geom17011@geo.aegean.gr

Abstract

Climate change is driven by several natural and anthropogenic factors and processes through the perturbation of the Earth's and atmosphere's energy budget [12]. Atmospheric aerosols, both natural and anthropogenic, remain one of the largest sources of uncertainty for climate change [1] with the aerosol vertical distribution being one of the causes of this uncertainty [23].

In the present work we present a global 3D climatology of aerosol optical depth (AOD) on a 2.5^0 x 2.5^0 horizontal and 500 m vertical resolution. The climatology is created using the CALIOP Level 2 Version 4.10 profile product, during both daytime and nighttime for an 11-year long period (2007-2017).

The results reveal significant spatial variability, with larger AOD over the Northern Hemisphere than the Southern and over land than oceans. On a mean annual level, greater aerosol load is observed above East Asia, the Arabian and Sahara Deserts and the Indian Subcontinent. The bulk of the aerosol load is mostly confined in the boundary layer. The interannual trends of the AOD are also estimated. The results indicate statistically significant (at the 95% level) increasing AOD trend over India and statistically significant decreasing trends in East Asia and the Arabian Peninsula. Smaller, albeit mostly statistically significant, decreasing trends are also found over Europe, the eastern United States and parts of South America. Our results are also compared against corresponding data from the MODIS - Aqua Dark Target - Deep Blue combined product (collection 061, level 3). Preliminary results reveal that the interannual trends based on CALIOP and MODIS AOD are in generally good agreement.

Keywords

Atmospheric aerosols, Desert dust, Satellite data, Vertical profiles

1. Introduction

The atmosphere is composed mostly of gases, but also contains liquid and solid matter in the form of particles, like clouds and aerosols [1]. Aerosols significantly affect the Earth's Energy Budget, while they interact, mainly, with solar radiation, through absorption and scattering. However, the concentration of aerosols and their properties are extremely variable in space and time.

However, it is pointed out that long-term studies using 3-D aerosol data are scarce, while being so much important. This study comes to fulfill this need, by using CALIOP data that come from the longest available aerosol database enabling vertical distribution.

The effect of aerosols on radiation may be (i) either direct, where the aerosols themselves scatter and absorb the solar and terrestrial (infrared) radiation, or (ii) indirect, where the aerosols modify the microphysical, optical and radiative properties of the clouds [28]. Moreover, there is also the semi-direct effect, which originates from the absorption of solar radiation by the aerosols that can modify the vertical profile of the temperature in the atmosphere, thus affecting the atmospheric stability and convection ([7]; [17]; [29]).

The interaction of aerosols with radiation, depend on their size, shape and chemical composition [1]. Atmospheric aerosols contain sulphate, nitrate, and ammonium elements, organic materials, metal oxides, hydrogen ions and water, while undergoing chemical and physical processes, resulting in a large and relatively rapid removal by sedimentation [1].

Aerosols are classified to different types, according to their origin, formation, shape and size. As to their origin, aerosols can be either natural or anthropogenic. Some examples of naturally occurring aerosols are desert dust, volcanic particles, and sea salt, while examples of aerosols of anthropogenic origin are urban-industrial aerosols and aerosols produced by building or construction activities. Biomass burning aerosols can be of either natural or anthropogenic origin. Worldwide, about 90% of aerosols are estimated to be of natural origin, while the remaining 10% are anthropogenic [27]. Most aerosols are located in the lower part of the troposphere, but their *effect* on radiation is *sensitive to their vertical distribution*. It is worth noting that the concentration of aerosols found in the troposphere has increased in recent years due to the increased anthropogenic emissions of aerosols and their precursor gases [28].

Aerosols are also classified in primary and secondary. The term primary refers to aerosols that are emitted directly into the atmosphere, while secondary aerosols are products of chemical reactions from precursor gases [1].

Finally, aerosols are separated according to their size, which helps to better understand their effects, not only on climate, but also on human health. The size of aerosols ranges between nearly 0.01 μm and 100 μm [24] and depends on the age of the plume (suspension) they form and their interaction [8]. Particles with a diameter of less than 2.5 μm belong to the fine mode, while particles with a diameter greater than 2.5 μm belong to the coarse mode. Large particles have high sedimentation rates and precipitate in the short term. Small particles represent a small percentage of the total mass of aerosols, but they are crucial for the effect on human health. Both types of aerosols have different sources of origin, and their transformation and removal mechanisms differ inside the atmosphere. These differences are identified both in their chemical composition and in their optical properties [24].

The aerosols are removed from the Earth's atmosphere by their aggregation with other particles and by the process of deposition on the Earth's surface. Moreover, it is mentioned that nucleation scavenging and conversion to cloud particles is also another mechanism. The deposition can be distinguished in dry deposition, which refers to the transfer to Earth' s surface due to gravity, and in wet deposition, which consists in removing the particles from the atmosphere, through their introduction into the precipitation [24].

In addition, it is noted that due to the short residence time of aerosols in the atmosphere and their different sources of origin, they are observed to be distributed unevenly, with maximum concentrations close to the sources [1].

In order to clarify and quantify the effect of aerosols on the climate, it is important to know their spatio-temporal distribution, as well as their chemical and optical properties [9]. In addition, another factor that strengthens this uncertainty is the incomplete knowledge of aerosols' vertical profiles and the errors that can be introduced due to the incorrect classification of the vertical superposition of clouds and aerosols ([14]; [2]).

The calculation of Aerosol Optical Depth (AOD) is based on the Beer – Lambert law

$$\frac{dF}{F_0} = -b_{ext} * dx$$

,where F_0 is the intensity of the incoming radiation flux, dF the change of the radiation flux due to extinction when traversing a path of length dx and b_{ext} is the extinction coefficient of the medium.

The result from integrating the above equation between two heights x_0 and $x(x_0 > x)$ is:

$$F = F_0 * e^{-\int_{x_0}^{x} b_{ext} * dx}$$

and

$$\tau_{ext} = \int_{x_0}^{x} b_{ext} * dx$$

Consequently the 2nd equation becomes:

$$F = F_0 * e^{-\tau_{ext}}$$

where τ_{ext} is the Aerosol Optical Depth.

2. Data and Analysis

Until recently, the available satellite aerosol optical properties data (e.g. MODIS) were limited to columnar values without being able to provide aerosol vertical distributions, which is of great interest. Such data have been made available thanks to Cloud-Aerosol Lidar with Orthogonal Polarisation (CALIOP) instrument onboard the Cloud-Aerosol Lidar and Infrared Pathfinder Satellite Observation (CALIPSO). In the present study the data from CALIOP are used in order to be able to investigate the vertical profile of the aerosols.

2.1. Input Data

CALIPSO observes the vertical distribution of aerosols and clouds since June 2006, through its primary instrument CALIOP [25]. CALIPSO is part of the A – Train (Afternoon Train), which also includes the Aqua, CloudSat and Aura satellites, flying in a 705-km sun-synchronous polar orbit providing global coverage between 82°N and 82°S, giving a 16-day repeat cycle, with an equator-crossing time of about 13:30 local solar time. ([25]; [31]). The orbit inclination of CALIPSO is at 98.2□ [30].

In this study, CALIOP Version 4.10 Level 2 Profile Product has been used. This product contains significant improvements in comparison with previous releases. The most important are the addition of a new subtype of aerosol named "dusty marine" and the separation and classification of aerosols located in the stratosphere [15]. The vertical resolution of CALIOP Level 2 data is 30 m up to the altitude of 8.2 km and 60 m for higher altitudes up to 20.2 km. The horizontal resolution is 5 km, however some layers are detected at coarser horizontal resolutions.

2.2. Analysis

In particular, the vertical profile of the extinction coefficient was used, from which the AOD was calculated. The data were averaged in space and time and monthly profiles with horizontal resolution of 2.5□ x 2.5□ and vertical resolution of 500 m (summing the raw resolution AOD data, up to 15 km) were calculated for the study period 2007-2017. For the calculation of the averaged profiles, we used the same quality control flags and criteria as Korras-Carraca et al., [16]. This averaging and quality screening methodology is similar to that described by Tacket et al., [25] applied in order to get the official level 3 product. Samples that do not match these criteria, were excluded from the analysis and were defined as missing values. Only samples corresponding to aerosols were used in the analysis. Samples that correspond to clouds were excluded and set as "missing value", while "clean air" samples were set as 0. The heights of the aerosol layers in this study correspond to values above mean sea level.

The data produced from the above methodology correspond not only to the profile, but also to the columnar AOD. In addition, the "Feature subtype" parameter has been used, which gives information on the type of aerosols in each layer, and the vertical and columnar profiles of Dust AOD were calculated. For this purpose, only categories classified by CALIOP as Dust, Polluted Dust and Dusty Marine were taken into account in the analysis. Data corresponding to the other aerosol classes was set as "missing value".

Subsequently, the mean (climatological) monthly, seasonal and annual data were calculated from monthly data, in the same spatial analysis. For the calculation of mean monthly climatological profiles, we set the restriction that data be available for at least 6 years. Mean climatological seasonal and annual profiles were calculated by averaging the mean monthly climatological profiles. In addition, the columnar AOD, for both total and dust aerosol subtypes, was calculated by summing the values of the profile, with the restriction that two-thirds of the profile has no "missing value".

Moreover, CALIOP AOD trends were calculated for the period 2007-2017. For this calculation, it was first necessary to calculate the time series of the anomalies for each month, in order to remove the seasonality (Time series Anomalies= Monthly Values - Mean (climatological) Monthly Values). Then, we checked whether the data follow normal distribution. If they follow normal distribution, a simple linear regression was applied for the calculation of the p-value (statistically significant areas). In the opposite case we used the non-parametric Mann-Kendall test. The p - value parameter examines whether the results extracted from its statistical test, either the linear regression or the Mann – Kendall tests, are statistically significant on the 95% confidence level. Finally, the Theil Sen method has been used in order to calculate the slope of the trend. The Theil Sen method has been chosen, as it is less sensitive to outliers, autocorrelation, and heteroscedasticity of errors in the input data, compared to the Least Squares method [10].

3. Results

3.1. Mean Annual Results

On a mean annual level, high AOD values are found in the northern hemisphere, mainly over land areas with significant sources of aerosols, such as deserts, as well as over oceans, such as the tropical North Atlantic and the Arabian Sea, where continental aerosols are transported. The highest AOD occurs in eastern Asia and India, with a range from 0.46 to 0.81, due to the significant presence of urban - industrial sources, biomass burning and dust aerosols. Relatively high AOD values, from 0.36 to 0.68, are observed in the arid and semi-arid regions of the Arabian Peninsula, North Africa and central Asia, where the aerosol load mainly consists of dust aerosols. In addition, over areas where biomass burning occurs (such as the southern and central Africa, as well as the Amazon Basin) [31, 13], the AOD is moderately high, from 0.28 to 0.46. Finally, medium to high AOD values (from 0.28 to 0.46) are observed in the tropical North Atlantic Ocean and the Arabian Sea, due to the advection of continental aerosols from adjacent arid and semi-arid areas.

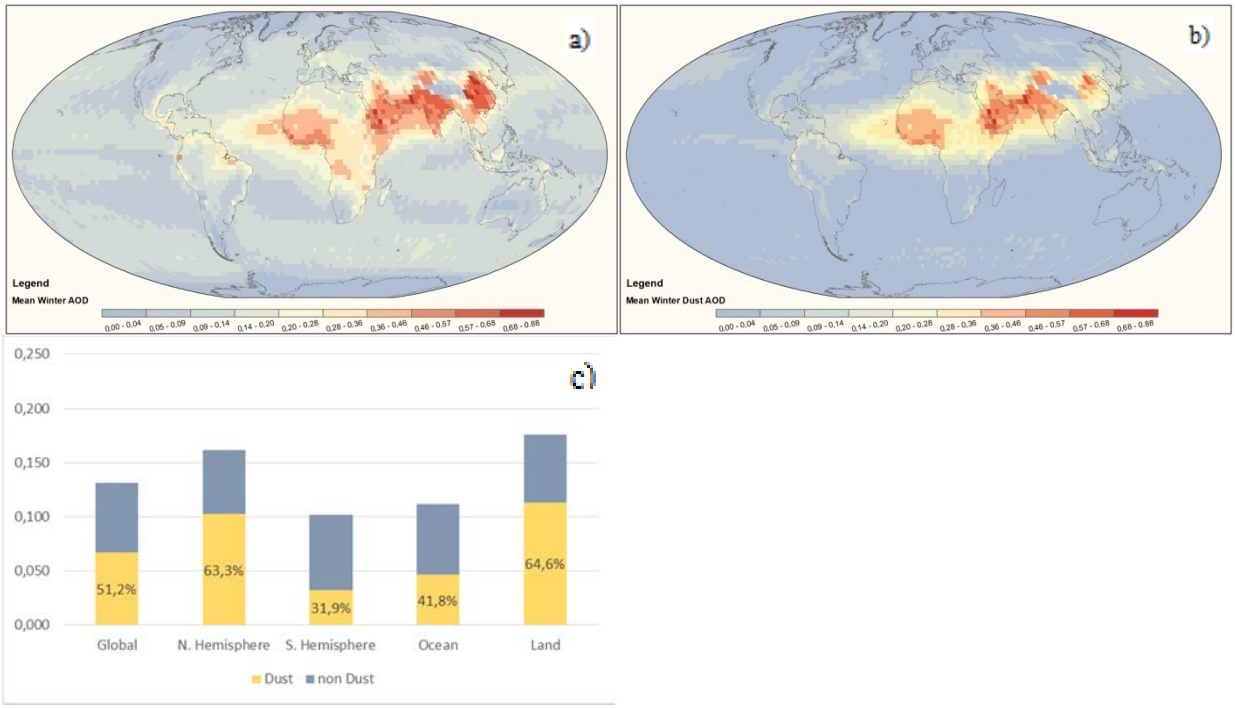

Fig. 1: a) Geographical distribution of the global mean annual AOD from CALIOP for the period 2007 – 2017, b) same as a) but for Dust AOD, c) Mean annual values of AOD and percentage of Dust AOD with respect to the total AOD

On a global scale the mean annual AOD is 0.13 of which 51 % is attributed to dust particles, according to the CALIOP classification scheme. In the Northern Hemisphere (NH), the annual average is 0.16 (63 % dust) and in the Southern Hemisphere is 0.10 (32 % dust) indicating a strong inter-hemispherical asymmetry caused by the existence of the world greatest deserts in the NH.

3.2. Seasonal Results

A significant seasonal variation is also evident with generally larger aerosol load, during boreal spring and summer compared to autumn and winter.

More specifically, in winter the regions with the highest AOD are located mainly in central Africa and the Sub-Sahel, with a range from 0.56 to 1.11. These high values are due to the extensive biomass burning that takes place during the winter (dry period) in the aforementioned regions and the transport of desert-dust particles from the Sahara, through the Harmattan winds [6, 3]. Large aerosol load, originating from central and northern Africa is transported over the Gulf of Guinea and the tropical North Atlantic Ocean, and contributes to the relatively high AOD observed above the aforementioned marine areas. High AOD values, from 0.42 to 1.11, are also observed inIndia and in south-east and east Asia, while medium AOD values from 0.14 to 0.42, are observed in the Arabian Peninsula and the east coast of South America. In the case of dust aerosols, a similar geographical distribution is observed, indicating that during winter in regions with a relatively high AOD, a significant

fraction of the aerosol load consistsof dust. More specifically, relatively high dust AOD values are observed in central Africa, the Sub-Sahel and East Asia, from 0.42 to 0.90, and medium values are observed in the Arabian Peninsula and India, with a range from 0.14 to 0.42.

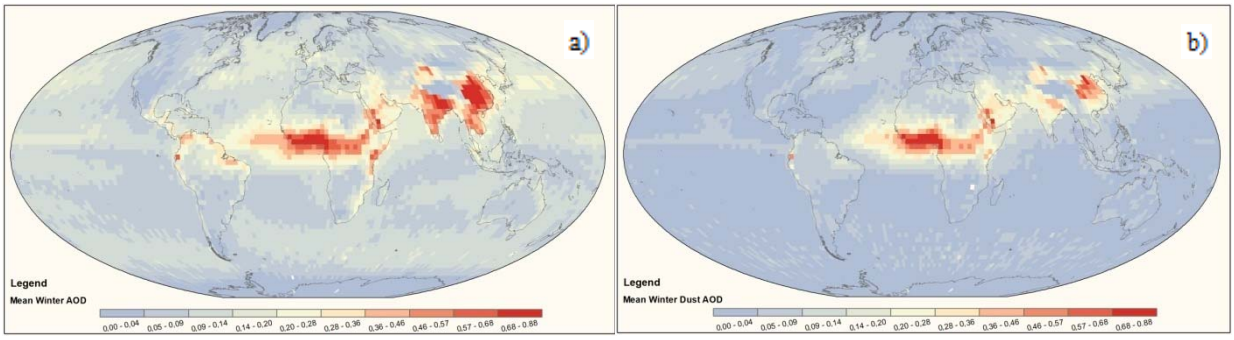

Fig. 2: a) Geographical distribution of the global mean Winter AOD from CALIOP for the period 2007 – 2017, b) same as a) but for Dust AOD

In spring, there is an increase in the AOD over most of North Africa, the Arabian Peninsula and Arabian Sea, India and part of central Asia (especially in the Taklamakan Desert), with values from 0.31 to 0.93. It is noted however, that the maximum AOD found in spring, is smaller than that of the winter (0.93 compared to 1.11). High AOD continues to prevail over the eastern Asia, with a range from 0.56 to 0.86. The increase of the AOD values during spring is due to a large increase in the dust activity in the Sahara, Arabian and the Taklamakan Desert ([18]; [21]). The increased presence of dust over vast areas of the planet, which mainly include central Africa, with values from 0.21 to 0.71, the Arabian Peninsula, from 0.42 to 0.86, India, from 0.56 to 0.86, and central Asia, mainly in the Taklamakan Desert, 0.56 - 0.86. In the tropical North Atlantic Ocean, a significant amount of dust is transported from the prevailing northeastern winds and observed values have a range from 0.21 to 0.56. Medium to high AOD observed in Central America are due to biomass burning [13] and range from 0.21 to 0.56.

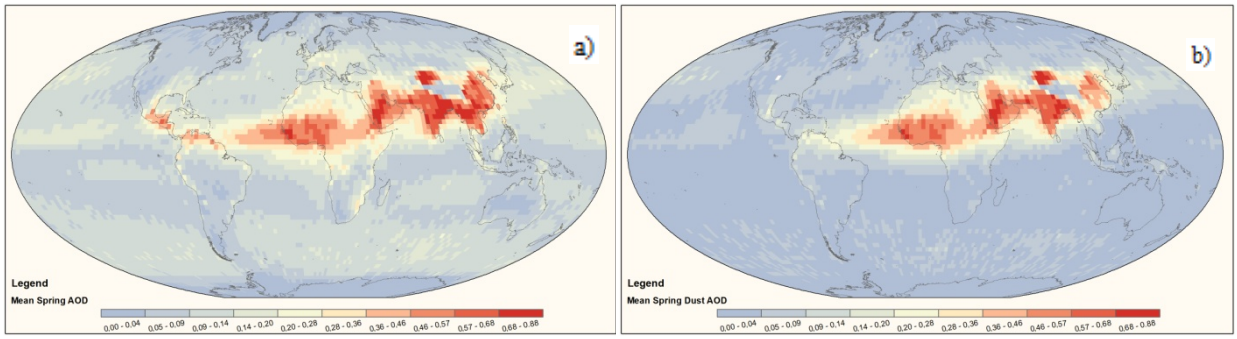

Fig. 3: a) Geographical distribution of the global mean Spring AOD from CALIOP for the period 2007 – 2017, b) same as a) but for Dust AOD

Summer is the season of maximum aerosol load over the majority of the world's regions, with AOD values reaching up to 1.43. Particularly high values are observed over the Sahara, from 0.42 to 0.86, and the Arabian desert, from 0.71 to 1.43, due to the strong dust activity in summer. Higher AOD are still observed in north-west India and more specifically in the Thar Desert and the Indus Valley, with a range from 0.86 to 1.43, due to the increased concentration of dust [20]. Significant aerosol load, mostly consisting of transported dust [21], is observed in the Arabian Sea with AOD from 0.86 to 1.43. Moreover, in the tropical North Atlantic Ocean, there is a northward latitudinal shift of the dust belt, following the latitudinal shift of the Intertropical Convergence Zone (ITCZ). In this region, the AOD values range from 0.21 to 0.71. In South Africa, the observed, particularly high, AOD values are due to the extensive biomass burning occurring in winter and spring of the southern hemisphere [11, 3, 5] which is the dry period and take values from 0.21 to 1.43.

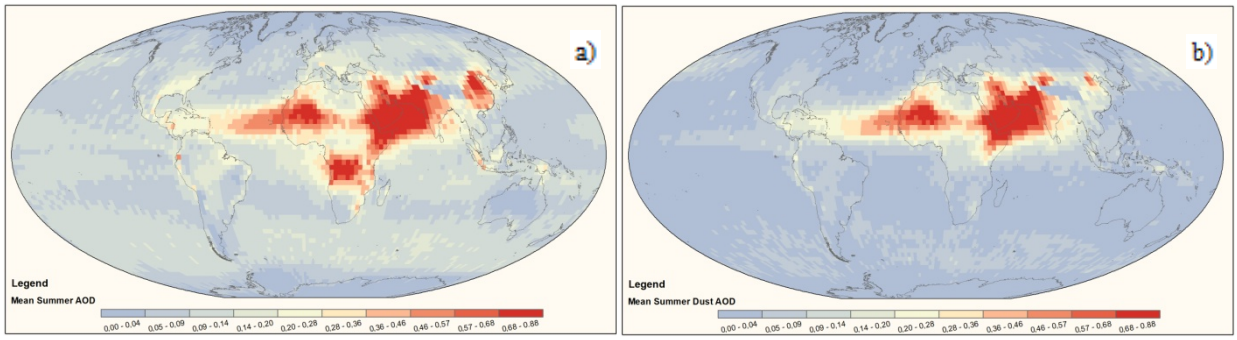

Fig. 4: a) Geographical distribution of the global mean Summer AOD from CALIOP for the period 2007 – 2017, b) same as a) but for Dust AOD

The smallest AOD compared to the other seasons is observed in autumn, with maximum values reaching up to 0.88. Medium to high AOD values are observed in regions where biomass burning is taking place, such as in south-east Africa (0.31 – 0.71) and in parts of South America (0.21 – 0.71), [26, 22]. The dust activity is significantly lower in the autumn, compared to spring and summer, so there is a clear reduction in AOD over the arid regions of the planet. Regions such as the Sahara, the Horn of Africa, the Arabian Peninsula, the Arabian Sea and south-east Asia have AOD values between 0.21 and 0.56, while in India, especially in Indus Valley and Thar Desert, AOD ranges from 0.42 to 0.71.

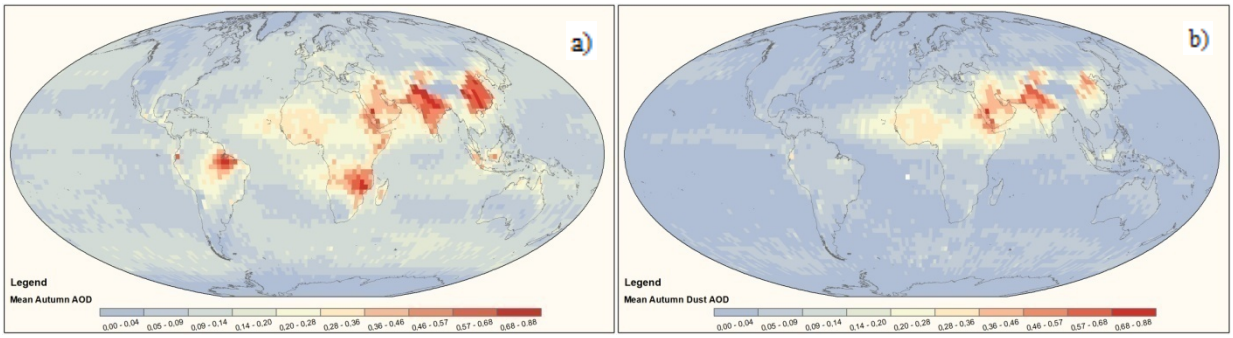

Fig. 5: a) Geographical distribution of the global mean Autumn AOD from CALIOP for the period 2007 – 2017, b) same as a) but for Dust AOD

3.3. Trends

In this section, total and dust AOD trends from 2007 to 2017 are presented. Regions, where trends are statistically significant, on a confidence level of 95%, are represented by a cross. In blue colors are depicted the downward trends, while in red the upward trends.

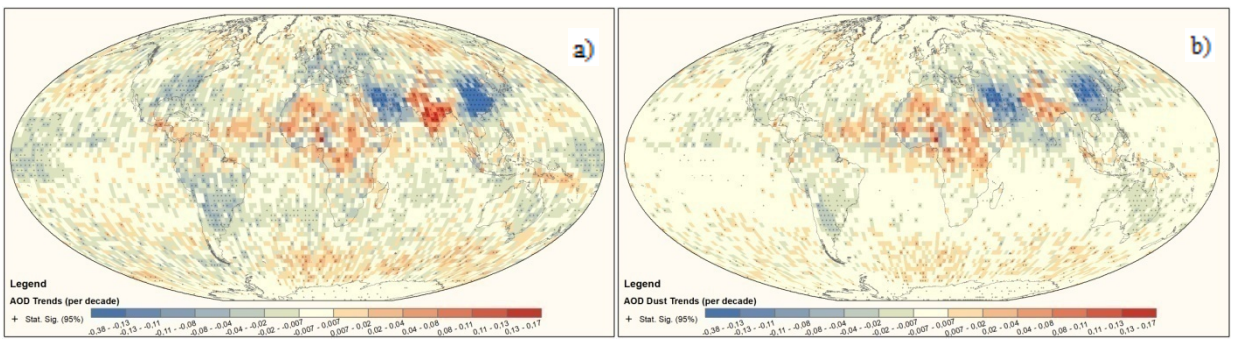

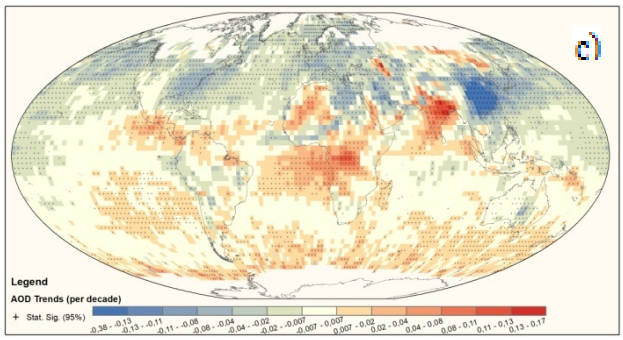

Fig. 6: a) Global AOD Trends from CALIOP, 2007 – 2017, b) the same as a) but for Dust AOD, c) Global AOD Trends from MODIS, 2007 – 2017

A statistically significant increasing trend (up to 0.17 per decade) has been observed over India, attributed possibly to the enhanced anthropogenic emissions [10]. On the other hand, statistically significant decreasing trends (up to 0.38 per decade) are observed in East Asia and the Arabian Peninsula. In case of Asia the decrease is largely associated with reduced anthropogenic emissions [19] and a decrease in the dust activity in central Asia, while for Arabian Peninsula it may be attributed to natural factors (precipitation, humidity, Monsoons etc). Smaller, albeit mostly statistically significant, decreasing trends are also found over Europe, the eastern United States and parts of South America. There are mostly due to the decrease in anthropogenic emissions [19] resulting from applied policies.

Slightly downward trends occur in eastern Australia (from 0.02 to 0.04 per decade), observed also in previous studies [19, 4] and the Central Pacific Ocean (from 0.02 to 0.08 per decade). Finally, statistically significant weak upward trends are also observed in the South Ocean and parts of Siberia ranging from 0.01 to 0.02 per decade.

Similar results also arise for the dust aerosol trends, except from Central Pacific Ocean region, where no significant dust AOD trends were recorded.

Moreover, CALIOP results are compared against corresponding data from MODIS - Aqua Dark Target - Deep Blue combined product (collection 061, level 3). The MODIS AOD data are regridded on a 2.5°×2.5° horizontal resolution. The interannual trends based on CALIOP and MODIS AOD are in generally good agreement. However, based on MODIS, generally decreasing trends are found over the North Hemisphere, except from India and parts of Siberia, and increasing trends are found in central Atlantic Ocean, over the Gulf of Guinea, and west of South America, in Pacific Ocean. In contrast with CALIOP there is no trend to be found in South America. The differences between MODIS and CALIOP can be partly explained due to the use of all available MODIS data (during each month) and not the common days between the two databases.

3.4. Vertical Profiles

In this section, the vertical profile profiles of total and dust aerosols, for six regions characterized by a high load of aerosols of both natural and anthropogenic origin, are presented. The selected regions, which are representative of different aerosol regimes, are North and South Atlantic Ocean, South Africa, India, East Asia and the Sahara - Middle East.

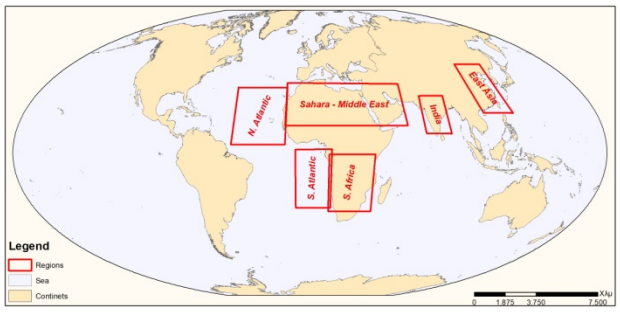

Fig. 7: Regions characterized by a high load of aerosols

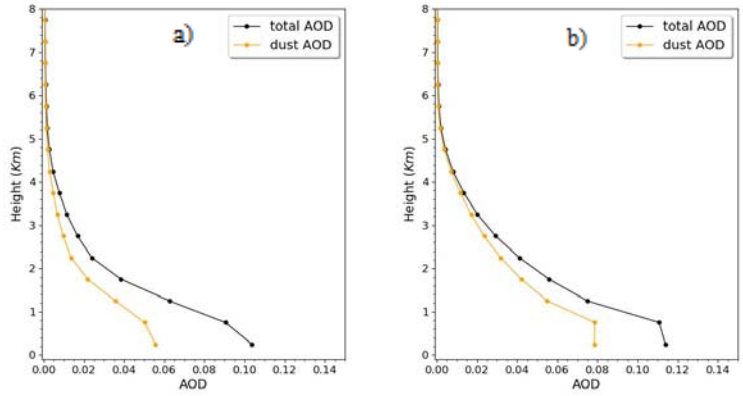

Fig. 8: a) Total Aerosol and Dust load for the East Asia, b) same as a) but for the India

For the East Asia and India, the largest aerosol load is observed in the boundary layer and the lower free troposphere, namely within the first 2.5 km. Dust particles contribute half as much to the total aerosol load in that area. The fraction of aerosols that do not correspond to the types of dust (CALIOP-based types is not shown here), comes from anthropogenic sources due to the intense industrial activity and the presence of large urban centers in the area. The relative contribution of dust particles over India is larger in the mid-upper troposphere, from 2 km and up, while aerosols reach up to higher altitudes (e.g. 3-3.5 km) over this world area.

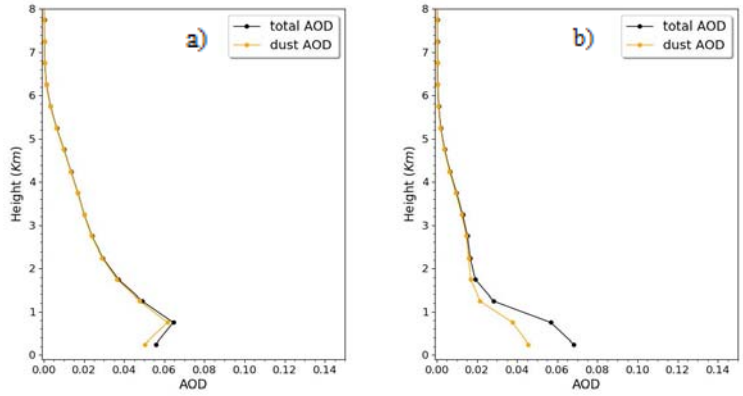

Fig. 9: a) Total Aerosol and Dust load for the Sahara - Arabian Peninsula, b) same as a) but for the tropical North Atlantic Ocean

Focusing on the Sahara and the Arabian Peninsula, relatively large AOD values are observed up to about 6 km. Most of the aerosols in these areas consist of dust particles. For the tropical North Atlantic Ocean, the largest load of aerosols is located up to 2km, and about half of them consist of dust aerosols transported from the Sahara Desert. At lower altitudes (within the boundary layer), a significant fraction of the aerosols consists of marine particles, while at higher altitudes the dust aerosols, which are advected from Sahara, are predominant.

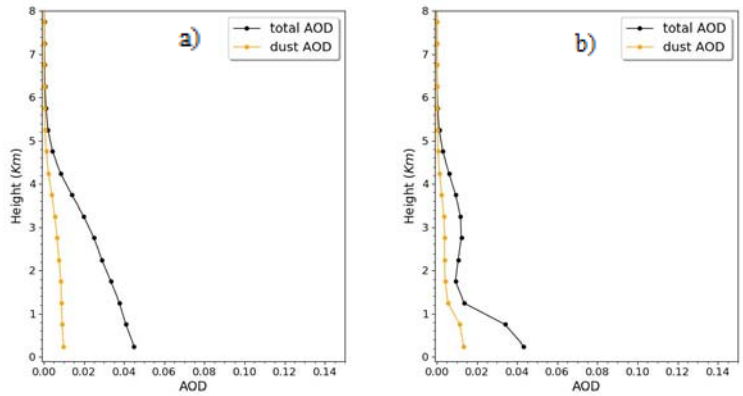

Fig. 10: a) Total Aerosol and Dust load for the South Africa, b) same as a) but for the tropical South Atlantic Ocean

As for South Africa, large aerosol load is observed from the surface up to 4 km. In this area biomass burning aerosols dominate. As a result, the contribution of dust particles to the total aerosol load is very low. Finally, in the tropical South Atlantic Ocean, a double maximum is observed in the vertical profiles, the main one within the atmospheric boundary layer (up to 1.5 km) and the secondary at a height of between 2 km and 4 km. Within the boundary layer, the aerosol load mainly consists of marine particles; while in the upper layers dominate biomass burning aerosols transported from the South Africa. The presence of dust is small.

4. Summary and Conclusions

In this study, the spatial distribution, the intraannual variation and interannual trends of the total, as well as dust aerosols, worldwide, using 11-year data from CALIOP have been investigated. Also, the mean annual vertical profiles for both total and dust aerosols, for six region of increased interest, were analyzed.

In detail, it is observed that larger AOD values are recorded over land areas. In particular, the largest annual AOD values are recorded in the regions of India and East Asia, where there are many natural and anthropogenic aerosol sources, as well as above deserts such as the Sahara, Taklamakan, Thar and the Arabian Desert, mainly characterized by dust aerosols. Marine areas with large AOD are the Arabian Sea and the tropical North Atlantic Ocean, due mainly to the export of aerosols from the adjacent continental areas, such as the Arabian Peninsula and northern Africa. Medium annual AOD values are recorded in South Africa and are mainly due to biomass burning.

The AOD generally has a large intraannual variation. Worldwide, higher AOD is observed during boreal spring and summer, compared to winter and autumn. In winter and spring, larger aerosol load consisting mainly of dust particles are recorded in regions of East Asia, India, the Arabian Peninsula and the Sahara Desert. In summer and autumn, apart from the aforementioned areas, high AOD values are observed in South Africa and the Amazon Valley, mainly due to biomass burning. In autumn, the world's smallest AOD values are recorded worldwide.

As far as trends are concerned, strong upward trends are recorded in India, mostly statistically significant, due to an increase in anthropogenic emissions.Upward trends are also observed over the Sahara Desert and North Atlantic Ocean. However, the upward trends recorded in the Sahara Desert, contradict previous research, perhaps due to different study period (2007-2017). Low upward statistically significant trends are also recorded in the Southern Ocean. Strong statistically significant downward trends are recorded in the Arabian Peninsula, which may depend on natural (meteorological) factors (changes in atmospheric circulation and rainfall), and East Asia, which depend on the reduction of anthropogenic emissions and the implementation of environmental protection measures. However, the downward trends observed in the Arabian Peninsula, contradict previous research, probably due to different study period. Low statistically significant downward trends are also recorded in the regions of Europe, North and South America, due to the reduction of anthropogenic emissions from the implementation of environmental protection measures. The interannual trends based on CALIOP and MODIS AOD are in generally good agreement. However, there are also some differences.

With regard to dust aerosols results, which are similar to those of total aerosols were recorded, with the largest proportion, however, not showing significant trends. Strong statistically significant trends in dust aerosols are observed in India (northern part, and Indus river valley), Sahara Desert and tropical North Atlantic Ocean. Strong downward statistically significant trends for dust aerosol are recorded in regions such as East Asia and Arabian Peninsula, as well as in the total aerosols. Low downward trends are recorded in parts of South and North America, as well as Australia.

Finally, with regard to the vertical profiles for total and dust aerosols, six areas of increased interest were examined: India, East Asia, Sahara - Middle East, tropical North Atlantic Ocean, tropical South Atlantic Ocean and the southern Africa. The bulk of the aerosol load is mostly confined in the boundary layer. However, in regions with significant aerosol sources, such as the Sahara and Arabian Deserts, India and East Asia we observe a large vertical extent of the aerosol layer with relatively large AOD up to the height of 6 km. At the South Atlantic the vertical distribution of AOD has a double maximum. The first maximum is observed in the marine boundary layer while the second is in the free troposphere and is associated with advected smoke from Southern Africa.

References

[1] Boucher, O., D. Randall, P. Artaxo, C. Bretherton, G. Feingold, P. Forster, V.-M. Kerminen, Y. Kondo, H. Liao, U. Lohmann, P. Rasch, S.K. Satheesh, S. Sherwood, B. Stevens X.Y. Zhang. Clouds and Aerosols. In: Climate Change 2013: The Physical Science Basis. Contribution of Working Group I to the Fifth Assessment Report of the Intergovernmental Panel on Climate Change In:Stocker, T.F., D. Qin, G.-K. Plattner, M. Tignor, S.K. Allen, J. Boschung, A. Nauels, Y. Xia, V. Bex P.M. Midgley (eds.) Cambridge University Press (2013)

[2] Choi, J.-O., Chung, C.E.: Sensitivity of aerosol direct radiative forcing to aerosol vertical profile. Tellus B (2014).doi:10.3402/tellusb.v66.24376.

[3] de Graaf, M., Tilstra, L.G., Aben, I., Stammes, P.: Satellite observations of the seasonal cycles of absorbing aerosols in Africa related to the monsoon rainfall. Atmos. Environ. (2010). doi:10.1016/j.atmosenv.2009.12.038

[4] de Meij, A., Pozzer, A., Lelieveld, J.: Global and regional trends in aerosol optical depth based on remote sensing products and pollutant emission estimates between 2000 and 2009. Atmos. Chem. Phys. Discuss. (2010). doi:10.5194/acpd-10-30731-2010)

[5] Edwards, D.P., Emmons, L.K., Gille, J.C., Chu, A., Attié, J.L., Giglio, L., Wood, S.W., Haywood, J., Deeter, M. N., Massie, S. T., Ziskin, D. C. Drummond, J. R.: Satellite-observed pollution from Southern Hemisphere biomass burning. J Geophys Res Atmos. (2006). doi:10.1029/2005JD006655

[6] Ginoux, P., Prospero, J.M., Gill, T.E., Hsu, C.N., Zhao, M.: Global-scale attribution of anthropogenic and natural dust sources and their emission rates based on MODIS Deep Blue aerosol products. Rev. Geophys (2012). doi:10.1029/2012RG000388.

[7] Grassl, H.: Possible changes of planetary albedo due to aerosol particles, in: Bach, W., Pankrath, J., Kellogg, W. (Eds.), Man's Impact on Climate. pp. 229–241. Elsevier, New York (1979).

[8] Hansell Jr, R. A., Reid, J. S., Tsay, S. C., Roush, T. L., Kalashnikova, O. V.: A sensitivity study on the effects of particle chemistry, asphericity and size on the mass extinction efficiency of mineral dust in the earth's atmosphere: from the near to thermal IR. Atmos. Chem. Phys. (2011). doi:10.5194/acp-11-1527-2011

[9] Hatzianastassiou, N., Matsoukas, C., Drakakis, E., Stackhouse Jr., P., Koepke, P., Fotiadi, A., Pavlakis, K., Vardavas, I.: The direct effect of aerosols on solar radiation based on satellite observations, reanalysis datasets, and spectral aerosol optical properties from Global Aerosol Data Set (GADS). Atmos. Chem. Phys. (2007a). doi:10.5194/acp-7-2585-2007

[10] Hsu, N., C., Gautam, R., Sayer, A., M., Bettenhausen, C., Li, C., Jeong, M., J., Tsay, S. – C., Holben, B., N.: Global and regional trends of aerosol optical depth over land and ocean using SeaWiFS measurements from 1997 to 2010. Atmos. Chem. Phys. (2012). doi:10.5194/acp-12-8037-2012

[11] Inness, A., Baier, F., Benedetti, A., Bouarar, I., Chabrillat, S., Clark, H., Clerbaux, C., Coheur, P., Engelen, R.J., Errera, Q., Flemming, J., George, M., Granier, C., Hadji-Lazaro, J., Huijnen, V., Hurtmans, D., Jones, L., Kaiser, J.W., Kapsomenakis, J., Lefever, K., Leitao, J., Razinger, M., Richter, A., Schultz, M.G., Simmons, A.J., Suttie, M., Stein, O., Thepaut, J.-N., Thouret, V., Vrekoussis, M., Zerefos, C., and the MACC team: The MACC reanalysis: an 8 yr data set of atmospheric composition. Atmos. Chem. Phys. (2013). doi:10.5194/acp-13-4073-2013

[12] IPCC: Climate Change 2013: The Physical Science Basis. Contribution of Working Group I to the Fifth Assessment Report of the Intergovernmental Panel on Climate Change.In Stocker, T.F., D. Qin, G.-K. Plattner, M. Tignor, S.K. Allen, J. Boschung, A. Nauels, Y. Xia, V. Bex P.M. Midgley(eds.) pp 1535, Cambridge University Press, Cambridge, United Kingdom and New York, NY, USA (2013).

[13] Kaufman, Y. J., Tanré, D., Boucher, O.: A satellite view of aerosols in the climate system. Nature (2002). doi:10.1038/nature01091

[14] Keil, A., Haywood J.M.: Solar radiative forcing by biomass burning aerosol particles during SAFARI 2000: A case study based on measured aerosol and cloud properties. , J. Geophys. Res. (2003). doi:10.1029/2002JD002315

[15] Kim, M.-H., Omar, A. H., Tackett, J. L., Vaughan, M. A., Winker, D. M., Trepte, C. R., Hu, Y., Liu, Z., Poole, L. R., Pitts, M. C., Kar, J., Magill, B. E.: The CALIPSO Version 4 Automated Aerosol Classification and Lidar Ratio Selection Algorithm.**Atmos.** Meas. Tech. Discuss.(2018)doi10.5194/amt-2018-166

[16] Korras – Carrasa, M., Pappas, V., Hatzianastassiou, N., Vardavas, I. Matsoukas, C.: Global vertically resolved aerosol direct radiation effect from three years of CALIOP data using the FORTH radiation transfer model.Atmos. Res. (2019). doi:10.1016/j.atmosres.2019.03.024

[17] Lu, Z., Streets, D. G., Zhang, Q., Wang, S., Carmichael, G. R., Cheng, Y. F., Wei, C., Chin, M., Diehl, T. Tan Q.,: Sulfur dioxide emissions in China and sulfur trends in East Asia since 2000. Atmos. Chem. Phys. (2010). doi:10.5194/acp-10-6311-2010

[18] Marinou, E., Amiridis, V., Binietoglou, I., Tsikerdekis, A., Solomos, S., Proestakis, E., Konsta, D., Papagiannopoulos, N., Tsekeri, A., Vlastou, G., Zanis, P., Balis, D., Wandinger, U., Ansmann, A.: Three-dimensional evolution of Saharan dust transport towards Europe based on a 9-year EARLINET-optimized CALIPSO dataset. Atmos. Chem. Phys. (2017). doi:10.5194/acp-17-5893-2017

[19] Mehta, M., Singh, R., Singh, A., Singh, N., Anshumali: Recent global aerosol optical depth variations and trends – A comparative study using MODIS and MISR level 3 datasets. Remote. Sens. Environ. (2016). doi:10.1016/j.rse.2016.04.004

[20] Proestakis, E., Amiridis, V., Marinou, E., Georgoulias, A. K., Solomos, S., Kazadzis, S., Chimot, J., Che, H., Alexandri, G., Binietoglou, I., Daskalopoulou, V., Kourtidis, K. A., de Leeuw, G., van der A, R. J.: Nine-year spatial and temporal evolution of desert dust aerosols over South and East Asia as revealed by CALIOP, Atmos. Chem. Phys. (2018). doi:10.5194/acp-18-1337-2018,2018.

[21] Prospero, J.M., Ginoux, P., Torres, O., Nicholson, S.E., Gill, T.E.: Environmental characterization of global sources of atmospheric soil dust derived from the NIMBUS7 TOMS absorbing aerosol product. Rev. Geophys (2002). doi:10.1029/2000RG000095

[22] Remer, L.A., Kleidman, R.G., Levy, R.C., Kaufman, Y.J., Tanre D., Mattoo, S., Martins, J.V., Ichoku, C., Koren, I., Yu, H., Holben, B.N.: Global aerosol climatology from the MODIS satellite sensors. J Geophys Res Atmos, 113 (2008). doi:10.1029/2007JD009661

[23] Samset, B. H., Myhre, G., Schulz, M., Balkanski, Y., Bauer, S., Berntsen, T. K., Bian, H., Bellouin, N., Diehl, T., Easter, R. C., Ghan, S. J., Iversen, T., Kinne, S., Kirkevåg, A., Lamarque, J.-F., Lin, G., Liu, X., Penner, J. E., Seland, O., Skeie, R. B., Stier, P., Takemura, T., Tsigaridis, K., and Zhang, K.: Black carbon vertical profiles strongly affect its radiative forcing uncertainty, Atmos. Chem. Phys., 13. (2013). https://doi.org/10.5194/acp-13-2423-2013

[24] Seinfeld, J.,H., Pandis, S., N.: Atmospheric Chemistry and Physics: From Air Pollution to Climate. A Wiley – Interscience Publication, John Wiley and Sons, INC, ed. 2nd, USA, Hoboken (2006).

[25] Tackett, J. L., Winker, D. M., Getzewich, B. J., Vaughan, M. A., Young, S. A., Kar, J.: CALIPSO lidar level 3 aerosol profile product: version 3 algorithm design. Atmos. Meas. Tech. (2018). doi:10.5194/amt-11-4129-2018

[26] Videla, F.C., Barnaba, F., Angelini, F., Cremades P, Gobbi GP.: The relative role of Amazonian and non Amazonian fires in building up the aerosol optical depth in South America: a five year study (2005–2009). Atmos. Res. (2013). doi:10.1016/j.atmosres.2012.10.026.

[27] Voiland, A. (2010). Aerosols: Tiny particles, big impact. Web.https://earthobservatory.nasa.gov/features/Aerosols [Accessed 14/1/2019].

[28] Watson, R., T., Albritton, D., L., Barker, T., Bashmakov, I., A., Canziani, O., Christ, R., Cubasch, U., Davidson, O., Gitay, H., Griggs, D., Houghton, J., House, J., Kundzewicz, Z., Lai, M., Leary,N., Magadza, C., McCarthy, J., J., Mitchell, J., F., B., Moreira, J., R., Munasinghe, M., Noble, I., Pachauri, R., Pittock, B., Prather, M., Richels, R., G., Robinson, J., B., Sathaye, J., Schneiber, S., Scholes, R., Stocker, T., Sundararaman, N., Swart, R., Taniguchi, T., Zhou, D.: Climate Change 2001: Synthesis Report. Contribution of Working Group I, II, and III to the Third Assessment Report of the Intergovernmental Panel on Climate Change [Dokken, D., J., Noguer, M., van der Linden, P., Johnson, C., Pan, J., and the GRID – Arendal Design Studio (eds.)]. Cambridge University Press (2001)

[29] Wang, X., Huang, J., Ji, M., Higuchi, K., 2008. Variability of East Asia dust events and their long-term trend. Atmos. Environ.doi:10.1016/j.atmosenv.2007.07.046

[30] Winker, D.M., Vaughan, M.A., Omar, A., Hu, Y., Powell, K.A., Liu, Z., Hunt, W.H., Young, S.A.: Overview of the CALIPSO Mission and CALIOP Data Processing Algorithms. J. Atmos. Ocean Technol. (2009). doi:10.1175/2009JTECHA1281.1

[31] Winker, D.M., Tackett, J.L., Getzewich, B.J., Liu, Z., Vaughan, M.A., Rogers, R.R.: The global 3-D distribution of tropospheric aerosols as characterized by CALIOP. Atmos. Chem. Phys. (2013). doi:10.5194/acp-13-3345-2013